Numerical simulation of wave-like nucleation events

Numerical simulation of wave-like nucleation events

Lang Yuan[1], Arvind Prasad[2], Peter D Lee[3] and David StJohn[2]

[1] Department of Mechanical Engineering, University of South Carolina, Columbia, SC, 29201, USA
[2] Centre for Advanced Materials Processing and Manufacturing, The University of Queensland, St Lucia, Queensland, 4072, Australia
[3]Department of Mechanical Engineering, Univesity College London, London, WC1E 6BT, UK

[1]langyuan@cec.sc.edu

Abstract. The Interdependence model [1] predicted that nucleation would occur in waves of events with regions of no nucleation in between each wave. The waves continue to form until nucleation covers the sample. The cause of this phenomenon was attributed to the formation of a nucleation-free zone which incorporates solute suppressed nucleation and inhibited nucleation zones. Recent real-time synchrotron x-ray studies by Prasad et al [2], Liotti et al [3] and Xu et al [4] have confirmed this hypothesis showing nucleation occurs in a step-wise fashion with a number of events occurring followed by little or no nucleation for a short period before another set of events occurs. A microscale solidification model that predicts diffusion-controlled dendritic growth has successfully shown the effect of the developing constitutional supercooling on the selection of nucleation events. In this study, we use this model to predict the solidification behaviour under the conditions experienced during these real-time synchrotron studies.

1. Introduction

Solidification processes that result in a microstructure of equiaxed grains are preferred with the associated better properties of the cast product and also ease of casting. Grain refinement using suitable inoculants is the standard practice in industry, but the exact mechanism of equiaxed grain formation leading to grain refinement still eludes us. An analytical model, the Interdependence Model [1], was developed which combines the particle and alloy chemistry characteristics, suggesting that while particles play a role in triggering a nucleation event, solute diffusion from an already growing neighboring grain provides constitutional supercooling (CS) that may also prevent nucleation events. The Interdependence model has been verified in different experimental scenarios as well as numerically [2,5,6].

Figure 1 shows a schematic that illustrates the Interdependence Model in the presence of a small thermal gradient (temperature increasing from left to right). The inoculant in the middle is triggered when there is adequate undercooling available. This CS is provided by the already growing grain on the left when it reaches a certain minimum size, rejecting solute ($k < 1$) as it continues to grow. The sum of the growth radius of the growing grain, x_{cs}, and the solute diffusion length, x_{dl}, creates a distance where nucleation is unlikely and is termed the Nucleation Free Zone (NFZ).

One of the natural extensions of the model is that wave-like nucleation can be predicted since the solute diffusion from the nucleated grain in the middle of the figure would provide the required CS for triggering the inoculant placed on the right. Such wave-like nucleation events have been observed in in-

situ experiments on different alloy systems performed at different X-ray synchrotron facilities – Al-Si [2], and Al-Cu [3,4]. These results reveal the nucleation wave-front as predicted by the Interdependence Model. Figure 2 shows the results from Prasad et al's work with Al-15Cu[7] .

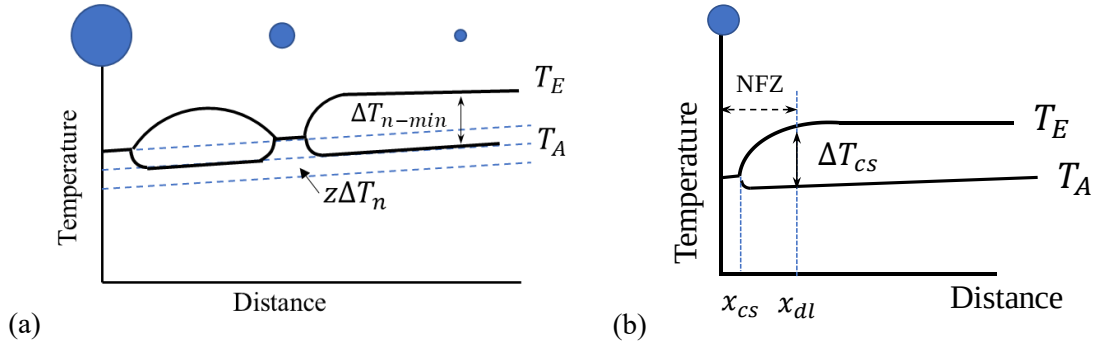

Figure 1. (a) The already growing grain on the left rejects solute and provides adequate constitutional supercooling (CS) to activate the inoculant in the middle triggering a nucleation event at a distance from the S-L interface. The now growing middle grain provides adequate CS for the rightmost inoculant to trigger another nucleation event. The process repeats and a cascade of nucleation events may be observed from left to right. T_A represents the melt temperature with a small thermal gradient from left to right. (b) In the Interdependence model the Nucleation Free Zone includes the radius of the growing grain and the diffusion length of the rejected solute as defined in [1].

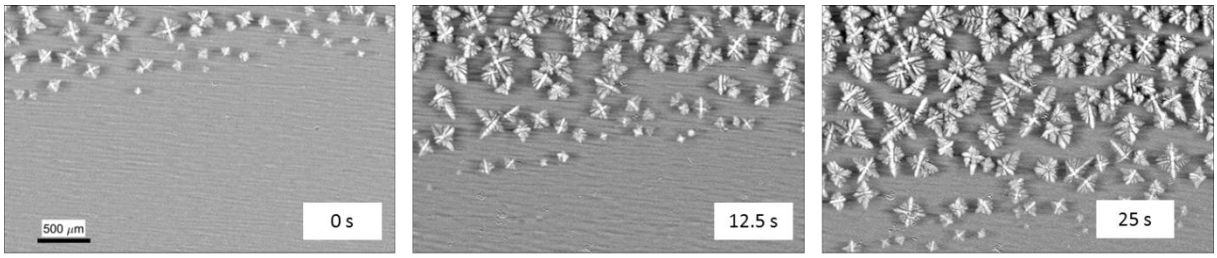

Figure 2. The cascading nucleation events observed during the in-situ X-ray synchrotron experiments with grain refined Al-15Cu. [adapted from [7]].

While the Interdependence Model is an analytical model, a numerical simulation technique is employed in this study to elucidate the effect of cooling rate and thermal gradient on the NFZ and thereby confirm the wave-like nucleation sequence. A cellular automaton based open source numerical model [8], which has been used to study the Interdependence model, was modified and applied to simulate the experimental conditions from the synchrotron experiments of [3] and [4].

2. Simulations of heterogeneous nucleation

The solidification model simulates nucleation events, dendritic growth with solute partitioning and diffusion. It has been validated against experiments in terms of the solute diffusion at the interface, the predictions of primary dendrite arm spacing, the columnar to equiaxed transition and freckle initiation during directional solidification processes [9–11]. The model implementations are not presented here, which were described in previous publications [12,13]. To evaluate the current model capability, a set of numerical simulations were calculated under the reported solidification conditions that have been examined through in-situ X-ray radiography by Xu et al.[4]. The experiments were performed with well-controlled cooling rates and thermal gradients. In addition, the observation direction is parallel to the gravity direction where convection and grain motion can be largely ignored. Thus, the experiments provide a reliable set of data for model comparison and further examination of nucleation behaviour.

Simulations are performed in a domain of 3×6 mm^2 ($x \times y$ to cover the field of view in the experiments (2.877×1.916 mm^2). Periodic boundary conditions in the x direction for both thermal and

solutal fields are applied to accommodate the wider experimental setup (5×50 mm^2). The extended dimension (6 mm vs. 1.919 mm) in the y direction allows the initial development of grains to get close to steady state where the observation most likely was done during the experiments. Since thickness (z) is 0.2 mm in the experiments, only 10 cells across the z direction were used in the simulation for thin 3D simulation envelopment to allow extra freedom of grain orientations. The simulation parameters are listed in Table 1. For nucleation, the Free Growth model [14], one of the most accepted models for heterogeneous nucleation of crystals with the addition of grain refiners, is simplified to a Gaussian distribution to account for stochastic nucleation as a function of the solute adjusted undercooling. The mean nucleation undercooling of 0.5K with a standard deviation of 0.1K was applied to control the nucleation events during directional solidification. The emphasis of the model is on constitutional supercooling due to segregation. Convection effects and the eutectic reaction are ignored.

Table 1. Simulation Parameters for Al-20wt%Cu alloy

Parameter	Unit	Value
Initial composition, C_0	wt%	20
Partitioning coefficient, k		0.14
Liquidus slope, m	K/wt%	-3.4
Liquidus Temperature, T_{liq}	K	875
Diffusion coefficient in solid, D_s	m/s^2	1.0e-12
Diffusion coefficient in liquid, D_L	m/s^2	4.65e-09
Cell size, d_{xyz}	M	5.0e-6

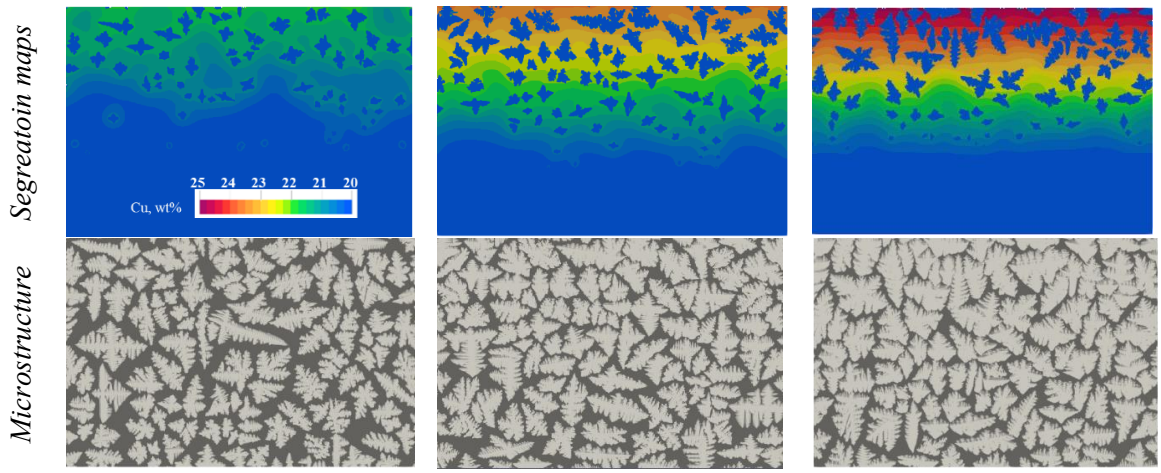

(a) R=0.5 K/s, G=5K/mm *(b) R=0.5 K/s, G=10K/mm* *(c) R=0.5 K/s, G=15K/mm*

Figure 3. Predicted segregation and microstrcture for inoculated Al-20wt% Cu alloy at 0.5K/s cooling rate under three different thermal gradients: (a) 5 K/mm, (b) 10 K/mm and (c) 15K/mm

Figure 3 shows the predicted segregation at the solidification front and the dendritic structures after grains fill the space during the directional solidification process for the cooling rate (R) of 0.5 K/s and increasing thermal gradients. With increasing thermal gradient, the withdraw velocity was reduced to keep the cooling rate constant. Note that the simulated domain was cropped to the same size as the experimental observation window and the maximum nucleation density (N_{max}) was set to 4.0E+12/m^3. The number of grains was also extracted from the simulations and plotted against the experimental data, as shown in Figure 4(a). Both the grain size and grain morphologies agree well with the experimental observations for the current conditions. This also indicates that the final grain size predicted from the current model agrees with the experimental results of Xu et al. [4]. The morphologies also correspond well with Liotti et al's experiment (Figure 2). A nucleation front is seen in all cases. The diffusion length which is proportional to D_l/v (where v is the solid-liquidus interface velocity), increases with increasing

thermal gradient. This increases the size of NFZ, resulting in a decrease in the number of grains, in other words, an increase of grain size.

Two other experimentally examined cooling rates (0.1 K/s and 0.025 K/s) were also simulated with the same model setup. However, to match the evolution of the number of grains, the maximum nucleation densities were reduced to 1.2E+12/m^3 and 0.8 E+12/m^3, respectively. With the same thermal gradient of 5K/mm, the number of grain reduces from ~110 to ~ 10 when the cooling rate decreases from 0.5K/s to 0.025K/s. Note that, within the same cooling rate, the model parameters remain unchanged.

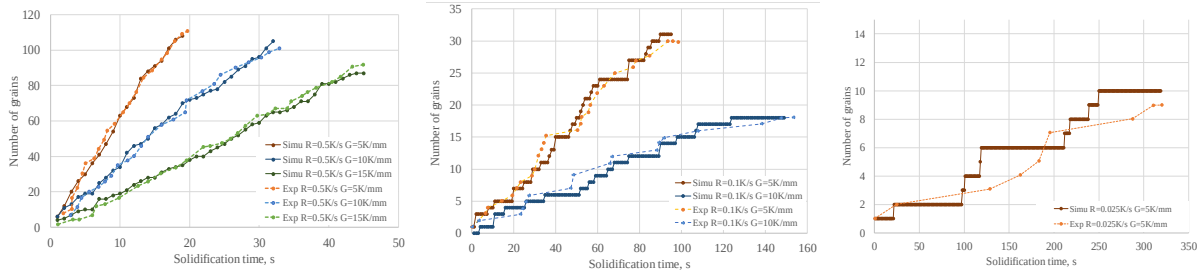

(a) *R=0.5K/s,* $N_m = 4.0E+12/m^3$ *(b) R=0.1K/s,* $N_m = 1.2E+12/m^3$ *(c) R=0.025K/s,* $N_m = 8E+11/m^3$

Figure 4. Evaluation of grain numbers for the same thermal gradeint (G = 5K/mm) at three different cooling rates, compared to the experimental data from the in-situ observations by Xu et al. [4]

3. Discussion

It has been proposed by the Free Growth model that dendrites are formed preferentially on larger nucleant particles first at relatively low undercooling and then progressively on smaller particles at a higher undercooling [14]. With inoculated Al alloys, a certain distribution of particle sizes is expected for the potential TiB_2 nucleants in the melt, where the population of small particles is much higher than that for the large particles. When the temperature starts to decrease, nucleation occurs first on large nucleants with low undercooling. The growing nuclei reject solute into the liquid for partitioning coefficients of $k < 1$. For a given thermal gradient, with a low cooling rate, solute has more time to diffuse compared to that with a high cooling rate giving the same thermal undercooling. This leads to a thicker solute segregation layer with higher solute concentration ahead of the solid-liquid interface and therefore lower CS. Based on the Interdependence Theory, nucleation events can be suppressed with lower CS, preventing nucleation on less-efficient nucleants. In contrast, with high cooling rate, a thinner solute segregation layer forms at the solidification front. The associated NFZ is reduced allowing nucleation on smaller nucleants which are more populous. Nucleation is further assisted by a faster heat extraction rate, which results in higher thermal undercooling. Based on this understanding, it implies that melts subjected to higher cooling rates have a higher potential to activate smaller nucleants with higher undercooling, compared to the situation when low cooling rates are applied. Moreover, Liotti et. al [3] observed that the mean and spread of undercoolings decrease with increasing cooling rate. This justifies the lower maximum nucleation density applied to the low cooling rate cases in the simulations which matched the experimental results. Since nucleation undercooling in the current simulations do not change, the increase of maximum nucleation density also reflects the increase of potential nucleants at higher cooling rates. This implies that a more sophisticated nucleation model that accounts for the actual size distribution of TiB_2 particles needs to be implemented to account for the variation of nucleation undercoolings.

In-situ X-ray studies have shown the wave-like nucleation under low cooling rates with low thermal gradients [2,3]. This is also observed in the simulations. From Figure 4(b) and (c), the incremental increase of nuclei number is in a step-wise manner which is enhanced at the lower cooling rate. The step-wise behaviour indicates that the formation of grains is paused for a certain period before a new set starts. As mentioned earlier, at lower cooling rate, the rate of CS development is reduced and the NFZ is extended. This requires additional heat extraction to increase the total undercooling and activate a

new set of particles, which leads to the pause in nucleation events. The new set of nuclei is well spaced from the previous sets due to the existence of NFZ, leading to the wave-like nucleation event as schematically shown in Figure 1(a). This phenomenon has been explained by the Interdependence model that includes the effect of the temperature gradient and the NFZ imposed by solute segregation resulting in the wave-like nucleation front in the refined alloys. The spatial distance of nuclei in the thermal gradient direction increases with the size of NFZ. Thus, the wave-like nucleation behaviour is observed more readily with large NFZ formed at low cooling rate. To better illustrate the wave-like nucleation event, a test case was run with R=0.01K/s and G=0.5K/mm, and shown in Figure 5. The nuclei are well spaced and grow in bands.

(a) t=150s *(b) t=200s* *(c) t=250s*

Figure 5. Wave-like nucleation for R=0.01K/s and G=0.5K/mm

For the same cooling rate (Figure 4(b)), the step-wise increments of grain number are more frequent at a high thermal gradient, indicating the promotion of the wave-like nucleation event. Figure 6(a) shows the solute profiles extracted at a steady state solidification front for G=10K/mm and G=15K/mm. A small difference in terms of solute distribution is observed along the length. (Note that these profiles can vary location by location, which are also affected by the surrounding grains. However, they can represent a typical scenario for each case). Neglecting the curvature undercooling and kinetic undercooling, the total undercooling for nucleation is plotted in Figure 6(b) by combining thermal and constitutional undercoolings.

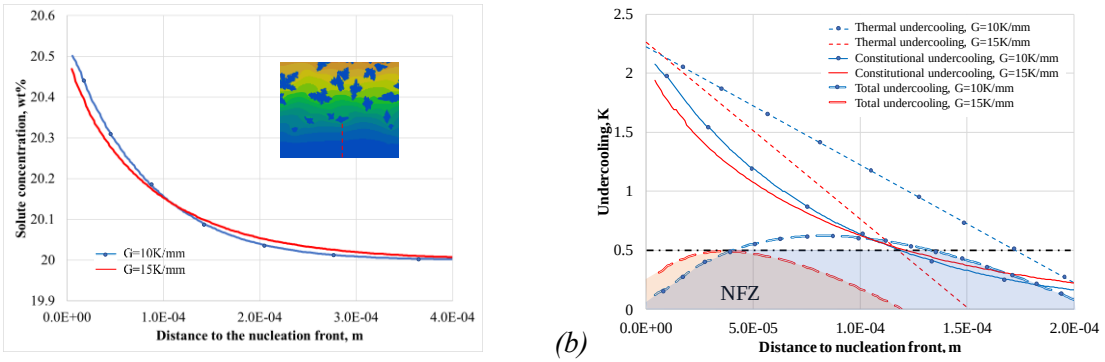

(a) *(b)*

Figure 6. Illustration of undercooling at the nucleation front: (a) solute profile extracted from simulation for R=0.5K/s. and (b) the illustration of NFZ.

As the thermal gradient increases, the total undercooling in the local melt decreases and the volume of the potential nucleation zone reduces. Assuming the inoculant undercooling of 0.5K, the entire length ahead of the solidification front for G=15K/mm is located under the limit, where there is less potential for grain formation and NFZ is expected throughout the length. Therefore, for the directional

solidification conditions [4], high thermal gradient increases the size of NFZ, which delays the nucleation events or totally prohibits nucleation. At lower thermal gradient some part of the total undercooling is above the inoculant undercooling limit and therefore exhibits a reduced NFZ. Thus, with increasing thermal gradient, the nucleation zone can be completely suppressed depending upon the cooling rate.

4. Conclusions

Wave-like nucleation events as predicted by the Interdependence Model have been revealed by in-situ X-ray experiments and validated by a microscale solidification model. The model agrees well with published experimental results in terms of both dendrite morphology and evolution of grain numbers by adjusting the maximum nucleation density, where the melt with a high cooling rate includes a larger number of potential nucleants of smaller size but in greater numbers. This indicates that the nucleation model in the simulation needs to be improved to account for the actual particle size distribution in a commercial grain refiner. Step-wise nucleation behaviour was predicted for the melts with low cooling rate. A demonstration case shows that the nucleation events are well-spaced, and the nuclei grow in bands. This agrees well with experimental observations that these wave-like nucleation events occur at low cooling rate. In addition, the nucleation events are also affected by the thermal gradient.

References

[1] StJohn D H, Qian M, Easton M A and Cao P 2011 The Interdependence Theory: The relationship between grain formation and nucleant selection *Acta Mater.* **59** 4907–21
[2] Prasad A, McDonald S D, Yasuda H, Nogita K and StJohn D H 2015 A real-time synchrotron X-ray study of primary phase nucleation and formation in hypoeutectic Al–Si alloys *J. Cryst. Growth* **430** 122–37
[3] Liotti E, Arteta C, Zisserman A, Lui A, Lempitsky V and Grant P S 2018 Crystal nucleation in metallic alloys using x-ray radiography and machine learning *Sci. Adv.* **4**
[4] Xu Y, Casari D, Mathiesen R H and Li Y 2018 Revealing the heterogeneous nucleation behavior of equiaxed grains of inoculated Al alloys during directional solidification *Acta Mater.* **149** 312–25
[5] Prasad A, Yuan L, Lee P D and StJohn D H 2013 The Interdependence model of grain nucleation: A numerical analysis of the Nucleation-Free Zone *Acta Mater.* **61** 5914–27
[6] StJohn D H, Prasad A, Easton M A and Qian M 2015 The Contribution of Constitutional Supercooling to Nucleation and Grain Formation *Metall. Mater. Trans. A* **46** 4868–85
[7] Prasad A, Liotti E, McDonald S D, Nogita K, Yasuda H, Grant P S and Stjohn D H 2015 Real-time synchrotron x-ray observations of equiaxed solidification of aluminium alloys and implications for modelling *IOP Conf. Ser. Mater. Sci. Eng.* **84** 12014
[8] The microstructural modelling of materials, http://www.imperial.ac.uk/engineering-alloys/research/software/
[9] Dai H J, Dong H B, D'Souza N, Gebelin J-C and Reed R C 2011 Grain Selection in Spiral Selectors During Investment Casting of Single-Crystal Components: Part II. Numerical Modeling *Metall. Mater. Trans. A* **42** 3439–46
[10] Dong H B and Lee P D 2005 Simulation of the columnar-to-equiaxed transition in directionally solidified Al–Cu alloys *Acta Mater.* **53** 659–68
[11] Karagadde S, Yuan L, Shevchenko N, Eckert S and Lee P D 2014 3-D microstructural model of freckle formation validated using in situ experiments *Acta Mater.* **79** 168–80
[12] Wang W, Lee P D and McLean M 2003 A model of solidification microstructures in nickel-based superalloys: predicting primary dendrite spacing selection *Acta Mater.* **51** 2971–87
[13] Yuan L and Lee P D 2012 A new mechanism for freckle initiation based on microstructural level simulation *Acta Mater.* **60** 4917–26
[14] Greer A, Bunn A, Tronche A, Evans P and Bristow D.2000 Modeling of inoculation of metallic melts: application to grain refinement of aluminium by Al–Ti–B *Acta Mater.* **48** 2823–35